A New Crystal Form Favored in Low Molecular Weight Biodegradable Poly(3-hydroxypropionate)

Bo Zhu,† Yong He,† Naoki Asakawa,† Haruo Nishida,‡ and Yoshio Inoue*,†

Department of Biomolecular Engineering, Tokyo Institute of Technology, Nagatsuta 4259-B-55, Midori-ku, Yokohama 226-8501, Japan, and Molecular Engineering Institute, Kinki University, 11-6, Kayanomori, Iizuka, Fukuoka, 820-8555, Japan

Received September 3, 2005; Revised Manuscript Received November 9, 2005

ABSTRACT: The crystalline structure of biodegradable poly(3-hydroxypropionate) (PHP) has been found to quite depend on the molecular weight (MW) and crystallization conditions. In particular, a new crystal form (the δ-form) has been successfully prepared by casting and optimal melt-crystallizing the low-MW PHP. The overwhelming growth of the δ-form in the cast low-MW PHP possibly arises from the conformational restriction of the intramolecular interaction between terminal groups. As for the melt-crystallization of low-MW PHP, the temperature of the melt (T_f) and the crystallization temperature (T_c) jointly decide the crystalline structure. It has been found that the T_f-dependent nucleation of the δ-form competes with T_c-dependent nucleation of the β- and γ-form and then plays a very important part in the T_f- and T_c-dependent polymorphism of PHP. With the aid of the FTIR analysis and the conformation prediction, the δ-form PHP are suggested to take on the 2_1 helix conformation rather than the trans one adopted by the γ-form PHP. Interestingly, although the δ-form has a higher melting temperature and is more thermally stable than the γ-form, no phase transition can be detected in the mixed phase of the δ-form and the γ-rich phase during heating.

Introduction

Ever since the end of the past century, the concerns about the environmental consequences of the large accumulation of polymer wastes have been much more enhanced, which greatly promotes the research on the biodegradable poly(hydroxylalkanoate)s (PHAs).[1] Up to date, a considerable body of knowledge on the enzymatic degradation of PHAs has been accumulated. With the great efforts and close cooperation of biologists and polymer scientists, the inherent relationships of the enzymatic degradation of PHAs to some solid-state properties, e.g., crystallinity[2] and crystal thickness,[3] have already been well revealed. However, the crystalline structure of PHAs, which possibly plays an important role in controlling biodegradation behavior, has not received the attention it deserves so far.

Polymorphism is a widespread phenomenon in polymers. Almost all crystalline polymers are polymorphic, if the precise conditions for the crystallization of the different forms can be found.[4] It is for very long time that the research on the polymorphism of polymers has been the hotspot of polymer science.[4,5] As is well-known, the multiformity of the intermolecular order as well as the intramolecular order is quite effective to decide the properties of polymeric materials, e.g., mechanical property, thermal property, electrical property, solvent resistance, and detrimental for the possible application and/or the processing of a polymeric material. However, few systematic investigations have been carried out to evaluate the polymorphism of biodegradable PHAs and its influencing factors. Until now, only limited results are available on crystal modifications of poly([R]-3-hydroxybutyrate) (PHB),[6] poly(L-lactide),[7] and poly(3-hydroxypropionate) (PHP).[8]

We think that the biodegradable PHP is an appropriate candidate to explore the relationship between the crystalline structure and the biodegradability, as PHP crystals show multiformity in both the conformation and the chain packing. It has been reported that PHP chains can be regularized into the 2_1 helix conformation in the α-form,[8a,d] in the trans one in the β-form by drawing the cast films at appropriate temperatures,[8a,b,d] or in the solution-grown γ-form lamellar (differ in the molecular arrangement from the projection to the *ab*-plane).[8b,c] However, a careful and systematic investigation on the spontaneous crystallization of various forms without loading external force is still absent until now, which is certainly indispensable to our next research on the biodegradation of PHP. Moreover, it is the PHP that builds up the basic chemical structural backbone of the typical bacterial poly(3-hydroxyalkanoate)s (P3HAs), one kind of the most important biodegradable PHAs. As all the P3HAs share the same backbone, i.e., the 3-hydroxypropionate (HP) skeleton, in terms of chemical structure, it is reasonable to expect that P3HAs will have identical conformations in the crystalline state. In fact, almost all the P3HAs can conform to the 2_1 helix and/or the trans in the crystalline phase, as predicted by the conformational calculation[9] and also well validated by related experiments.[6,8,10] It is quite expected that the research on polymorphism of PHP would shed light on the crystallization and the biodegradation of the bacterial P3HAs and further the relationship between them.

In our previous work,[11a] we have studied the crystallization temperature (T_c)-dependent polymorphic crystallization and melting of the high-molecular-weight PHP. In fact, besides T_c, the molecular weight (MW) and the temperature of the melt (T_f) have been found to greatly affect the crystallization of PHP, part of which has ever been preliminarily reported by us most recently.[11b] In this work, a careful and detailed investigation will be carried out to reveal the effect of MW and T_f on the crystallization of PHP. It is found that a new crystal form is favored in the low-molecular-weight PHP, which, to our knowledge, has not been reported in the literature. For understanding the molecular weight and T_f-dependent polymorphism

* To whom all correspondence should be addressed: Tel +81-45-924-5794; Fax +81-45-924-5827; e-mail yinoue@bio.titech.ac.jp.
† Tokyo Institute of Technology.
‡ Kinki University.

10.1021/ma051922v CCC: $33.50
Published on Web 12/09/2005

Table 1. Characteristics of PHP Samples and Their Fractions

sample code	wt (%)	M_w ($\times 10^{-5}$)	M_n ($\times 10^{-5}$)	M_w/M_n	crystal
PHP87K	100	2.13	0.87	2.45	$\beta+\gamma+\delta$
f1	9.5	4.86	3.63	1.34	γ
f2	45.5	2.65	1.92	1.38	$\beta+\gamma$
f3	21.5	1.78	1.29	1.38	$\beta+\gamma$
f4	8.5	0.90	0.76	1.19	$\beta+\gamma$
f5	5.5	0.66	0.56	1.17	$\beta+\gamma+\delta$
f6	9.5	0.29	0.15	1.93	δ
PHP70K	100	1.42	0.70	2.03	γ
f1	15.6	2.76	2.38	1.16	γ
f2	43.9	1.74	1.30	1.34	$\beta+\gamma$
f3	14.3	1.17	0.91	1.29	$\beta+\gamma$
f4	9.2	0.69	0.58	1.19	$\beta+\gamma$
f5	5.9	0.50	0.45	1.12	$\beta+\gamma+\delta$
f6	11.1	0.29	0.24	1.20	δ
PHP56K		1.22	0.56	2.17	$\gamma+\delta$
PHP18K		0.45	0.18	2.48	δ

of PHP, a variety of research techniques are used. The crystal structures of the cast PHPs with various MWs and those of the melt-crystallized ones melted at different T_fs are studied by X-ray diffraction and Fourier transform infrared spectra (FTIR). Further, the growth kinetics and morphology of various crystals are studied by the polarized optical microscopy (POM). Finally, the time-resolved FTIR is employed to investigate the molecular origin of the T_f-dependent polymorphism during the crystallization and subsequent melting processes.

Experimental Section

Materials. Four kinds of chemically synthesized PHPs (PHP18K: $M_n = 1.8 \times 10^4$, $M_w/M_n = 2.48$; PHP56K: $M_n = 5.6 \times 10^4$, $M_w/M_n = 2.17$; PHP70K: $M_n = 7.0 \times 10^4$, $M_w/M_n = 2.03$; PHP87K: $M_n = 8.7 \times 10^4$, $M_w/M_n = 2.45$) prepared by a ring-opening polymerization of propiolactone were kindly supplied by Tokuyama Co. (Japan) and was purified from chloroform solution by precipitation in heptane.

PHP87K and PHP70K, at a concentration of 5 mg/mL, were fractionated into six fractions with different molecular weights, using chloroform (solvent) and heptane (nonsolvent). The molecular characteristics of PHP samples and their fractions, determined by GPC, are tabulated in Table 1.

Preparation of Polymorphic PHPs. The films of original PHPs and their fractions were prepared by casting their chloroform solutions with an appropriate concentration, 10 mg/mL, on the Teflon dishes. The solvent was allowed to evaporate slowly at 25 °C for at least 1 week before measurements. It should be noted here that all the cast samples are prepared at the same time and under the same condition in order to eliminate the effects of volatilization rate utmost.

Melt-crystallized PHPs were compression-molded under 5 MPa at a given temperature for 3 min (containing 1.5 min of post-annealing without pressure), then quenched to a desired crystallization-temperature, and annealed for a time to generate polymorphic crystalline phase. Similar thermal treatments were also employed to prepare the melt-crystallized polymorphic samples in the POM, DSC, and the in-situ FTIR measurements but without pressure loading.

Analytical Procedures. Wide-angle X-ray diffraction (WAXD) measurements were carried out on a Rigaku RU-200 (Rigaku Co., Tokyo, Japan), working at 40 kV and 200 mA, with Ni-filtered Cu Kα radiation ($\lambda = 0.154\,18$ nm). Scans were made between 2θ's of 5°−60° at a scanning rate of 1° min^{-1}.

Microphotographs were recorded by a FUJIX digital camera HC-2500 3CCD (Fuji Film Co., Tokyo, Japan). The radius of growing spherulites was monitored by taking microphotographs during appropriate time intervals before spherulite impingement. Plotting the spherulite radius against the growth time, a straight line was obtained. The average radial growth rate was taken as its slope.

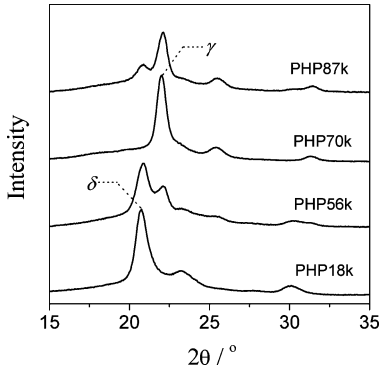

Figure 1. WAXD patterns of cast PHP with different molecular weights.

The transmission FTIR measurements were carried out on an AIM-8800 automatic infrared microscope (Shimadzu Co., Kyoto, Japan). The transmission FTIR spectra with an accumulation of 16 scans were in situ registered during the whole crystallization of PHPs and the subsequent heating at a constant rate of 1 °C/min. All the IR spectra are registered at a resolution of 2 cm^{-1}.

The melting of the polymorphic PHPs was also registered by a Pyris Diamond DSC instrument (Perkin-Elmer Japan Co., Tokyo, Japan). The scales of temperature and heat flow at different heating rates were calibrated using an indium standard with nitrogen purging. All the DSC samples have a mass of about 5 mg and were heated at a constant rate.

Results

δ-Form Crystal Favored in Low-Molecular-Weight PHP. In Figure 1 are shown the X-ray diffraction profiles of the cast films of four kinds of PHPs, which differ in the molecular weight (MW) but have a similar film thickness of about 100 μm. The cast PHP70K shows three diffraction peaks with 2θ's at 22.1°, 25.4°, and 31.5°, which can be assigned to the reflection of the γ-form crystal.[8c] For PHP56K, the diffraction peaks characteristic of the γ-form are weakened, indicating the reduction of the γ-form in the crystalline phase. In addition, three new diffraction peaks can be clearly observed at 20.7°, 23.3°, and 30.0°, any of which, however, cannot be assigned to the reflection of any known crystal form, i.e., the α-, β-, and γ-form, of PHP.[8] With further lowering MW to 1.8×10^4, only these unknown diffraction peaks remain and are enhanced. It is obvious that the three new diffraction peaks should correspond to an unknown crystalline structure of PHP, denoted as the δ-form in our previous preliminary report.[11b]

As the cast conditions are strictly controlled to be the same for all PHPs, the difference in the crystalline structure among PHP70K, PHP56K, and PHP18K should be due to that in MW. Namely, it seems that lower MW favors the growth of the δ-form. However, as shown in Figure 1, both the γ- and δ-form crystals can be detected in the cast PHP87K film, whose MW is the highest among the four PHPs. In addition, the appearance of a weak diffraction peak at 22.9° likely indicates that a small amount of the β-form also reside in the cast PHP87K. Thus, it seems hesitating to draw an unambiguous conclusion on the effect of the MW. To explain this confliction, the molecular characteristics are inspected for the four PHPs. As described in the Experimental Section, the distribution index of MW (M_w/M_n) of PHP87K is 2.45, which is wider than that, i.e., 2.03, of PHP70K. If the MW affects the crystalline structure of PHP, the MW distribution also does.

Molecular Weight Dependence in Fractionated PHPs. The solvent−nonsolvent fractional precipitation was applied to resolve PHP87K and PHP70K into a series of fractions with

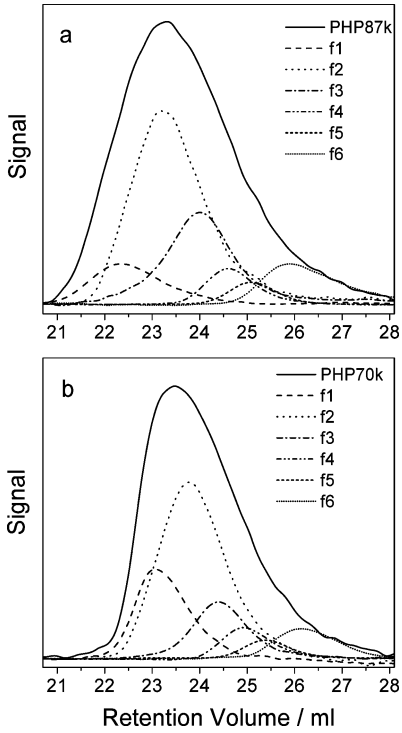

Figure 2. GPC curves of PHP87K, PHP70K, and their fractions.

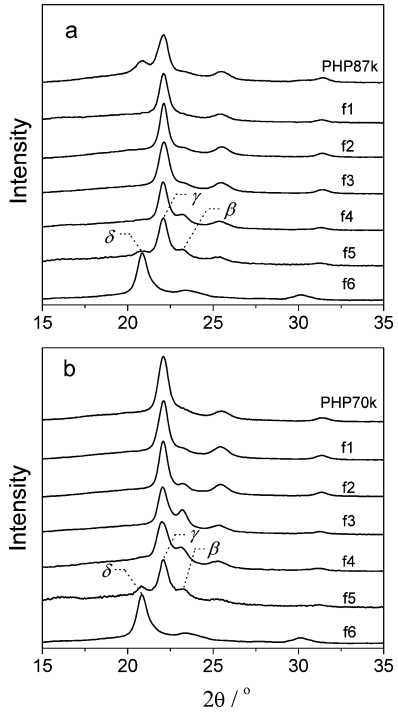

Figure 3. WAXD patterns of cast PHP87K, PHP70K, and their fractions.

different MWs. Figure 2 shows the GPC curves of PHP87K and PHP70K and their fractions, where the area under the curve denotes the relative weight content of the PHP sample if the area corresponding to the original PHP is normalized. Obviously, a shift of the retention volume toward larger value occurs for fractions of both PHP87K and PHP70K in the order of f1 < f2 < f3 < f4 < f5 < f6, revealing that the fractionation of MW did take place, where the larger value of "*n*" in the fraction code "f*n*" means the higher volume ratio of nonsolvent to solvent used here. Moreover, in comparison with the PHP87K and PHP70K, the GPC curves of their fractions are much narrower, indicating the narrower distribution of MW for the fractions than that for the original PHPs. Tabulated in Table 1 are the molecular characteristics of the original PHPs and their fractions, measured by GPC. It is noted that most of the fractions have a MW distribution below 1.4. Therefore, with using these fractions, the effect of MW distribution on the crystallization is expected to be negligible.

In Figure 3 are shown the X-ray diffraction patterns for PHP87K, PHP70K, and their fractions. As expected, both the crystalline structures of the PHP87K fractions and those of the PHP70K fractions exhibit a monotonic dependence on the MW. That is, with lowering MW, the crystallization of PHP occurs in the γ-, β-, and finally the δ-form. However, it should be noted that the β-form crystal has never been the predominant phase no matter how much the MW value of the fraction is. The dependence of the crystalline structure of PHP on the MW value is also listed in Table 1. It is clear that the critical MW value for the phase inversion from the γ- to β-form and that from the β- to the δ-form crystal are around 1.9×10^5 and 5.6×10^4, respectively.

Dependence on Temperature of the Melt. The X-ray diffraction profiles of the PHP18Ks crystallized at 70 °C after melted at a variety of T_fs are shown in Figure 4a. When melted at 130 °C, the PHP18K should crystallize in a γ-rich phase contaminated by a small amount of the β-form, as it shows a strong diffraction pattern characteristic of the γ-form (22.1°, 25.4°, and 31.5°)[8c] and a weak one characteristic of the β-form

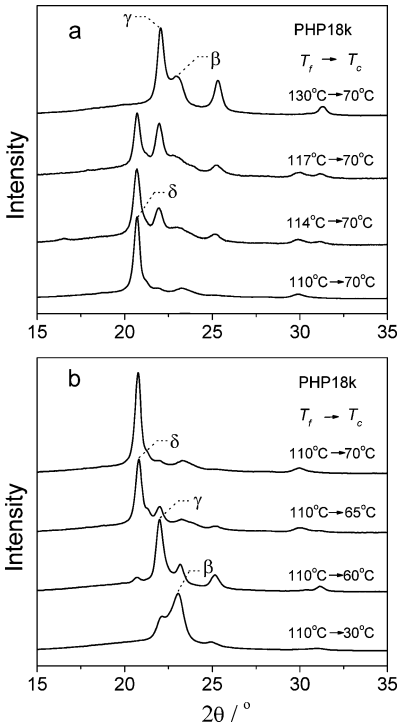

Figure 4. (a) WAXD patterns of PHP18Ks crystallized at 70 °C after being quenched from 130, 117, 114, and 110 °C and (b) those crystallized at 70, 65, 60, and 30 °C after being quenched from 110 °C.

(22.9°).[8a,b,d] When the T_f is lowered to or below 117 °C, the diffraction pattern of the γ-form is much weakened, while that of the δ-form (20.7°, 23.3°, and 30.0°) emerges and will be enhanced with further decreasing the T_f. Once the T_f is lowered to 110 °C, the δ-form is found to be overwhelmingly preponderant in the crystalline phase.

Dependence on Crystallization Temperature. The effect of the crystallization temperature (T_c) on the crystalline structures of PHP18K melted at 110 °C was also investigated. In

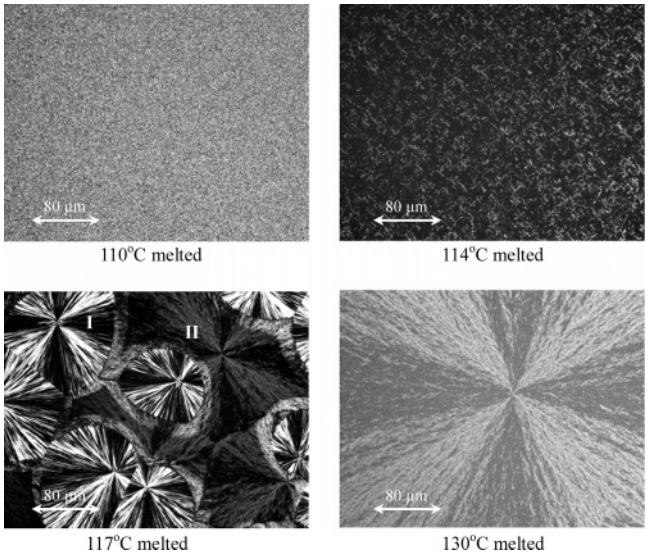

Figure 5. Optical microphotographs of spherulites in PHP18Ks crystallized at 70 °C after quenched from 110, 114, 117, and 130 °C. Type I and II spherulites correspond to the δ-form and the γ-rich phases, respectively.

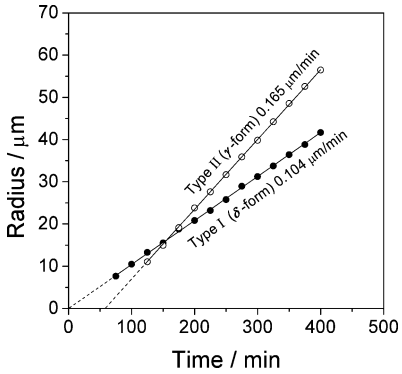

Figure 6. Radius of type I (δ-form) and II (γ-form) spherulites growing in PHP18K at 70 °C after being quenched from 117 °C as a function of time.

Figure 4b are the X-ray diffraction profiles for PHP18Ks crystallized at a variety of T_cs from 30 to 70 °C after melting at 110 °C. Obviously, with decreasing the T_c from 70 to 60 °C, the crystalline structure changes from an almost pure δ-phase to a γ-rich phase. However, with further decreasing the T_c to 30 °C, the β-form crystal becomes dominant.[11a]

Spherulite Growth and Unique Morphology. A POM examination was carried out to investigate the origin of the T_f-dependent polymorphism. In Figure 5 are shown the spherulite morphologies of the PHP18Ks melt-crystallized at 70 °C after melted at various T_fs. It is found that the spherulite density decreases drastically with increasing the T_f from 110 to 130 °C, indicating the nuclei density quite depends on the residual thermal history. Possibly, the growth of spherulite possibly initiates from some residual crystal fragments or ordered chain structures surviving at low T_fs.

The most interesting results found here is that two types of spherulites grow synchronously at 70 °C in the PHP18K film quenched from 117 °C, as shown in Figure 5. They have very different morphologies, although both exhibit a radially aligned sheaflike texture and a negative birefringence. In detail, one population of spherulites is compact and clear (type I), while the other one is very coarse and open (type II). The radial growth rates of two types of the spherulites can be measured via monitoring the growth of spherulite. In Figure 6 are shown the

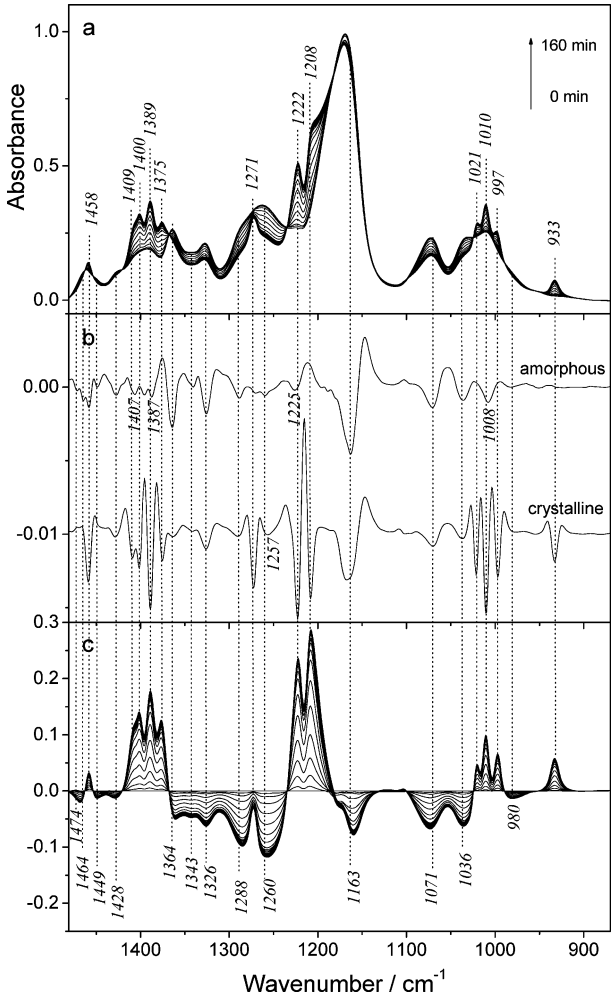

Figure 7. (a) Time-resolved FTIR spectra in the 1500−850 cm^{-1} range of PHP18K isothermally crystallizing at 70 °C after being quenched from 110 °C. (b) Second derivatives of the spectra registered at the beginning (0 min) of the crystallization and after crystallization of 160 min. (c) Difference spectra calculated by subtracting the initial amorphous spectrum from (a).

plots of the spherulite radius of the type I and II as a function of time. From Figure 6, the growth rates, i.e., the slopes of the plots, are calculated to be 0.104 and 0.165 μm/min for the type I and II, respectively, with a difference by a factor of almost 1.65.

To clarify the origin of the different spherulites, an infrared microscope is used. An appropriate area of the square aperture for the registration of FTIR spectra is set to match the size of the spherulite. It is found that the IR spectra of the type I and II spherulites (not shown) are very different, which are the same as those of the δ-form and the γ-rich phase, respectively.

Crystallization of δ- and γ-Form. In Figure 7a are shown the FTIR spectra for the δ-form PHP registered at 70 °C in situ during the isothermal crystallization of the PHP18K quenched from 110 °C. Obviously, with the crystallization proceeding, many new bands appear and are further enhanced in the 1500−850 cm^{-1} region. However, the IR absorption bands severely overlap with each other, especially for those of the amorphous PHP, making it difficult to accurately define these IR bands. Thus, the second derivatives of the spectra registered at the beginning (0 min) and after the crystallization of 160 min have been calculated, and the results are shown in Figure 7b. It is clear that the amorphous PHP shows distinctive IR absorptions at 19 positions, i.e.,1474, 1464, 1458, 1449, 1428, 1407, 1387,

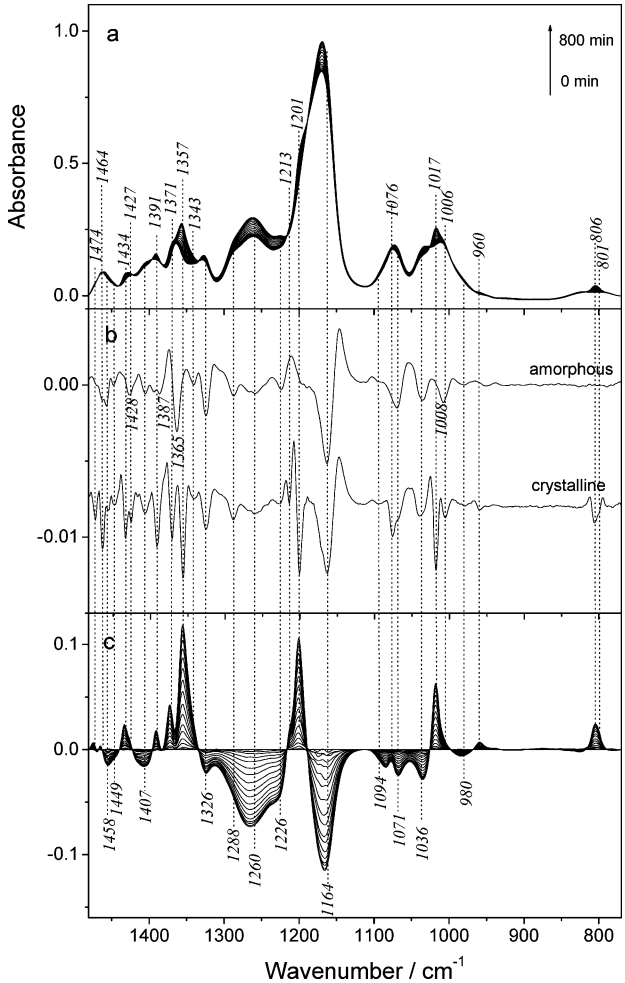

Figure 8. (a) Time-resolved FTIR spectra in the 1500−750 cm^{-1} range of PHP18K isothermally crystallizing at 70 °C after being quenched from 130 °C. (b) Second derivatives of spectra registered at the beginning of the crystallization (0 min) and after the crystallization of 800 min. (c) Difference spectra calculated by subtracting the initial amorphous spectrum from (a).

1364, 1343, 1326, 1288, 1271, 1260, 1225, 1163, 1071, 1036, 1008, and 980 cm^{-1}. Therefore, in the spectra of the δ-form PHP, except for these amorphous bands, the other ones at 1458, 1409, 1400, 1389, 1375, 1222, 1208, 1021, 1010, 997, and 933 cm^{-1} should be of the crystalline origin. For the aim of the confirmation, the difference spectra have been calculated by subtracting the initial amorphous spectrum from the time-resolved spectra, as shown in Figure 7c. It is reasonable to note that all the crystalline bands are enhanced with the time elapsing. Interestingly, the amorphous band at 1458 cm^{-1} is also enhanced during the crystallization. In addition, no distinctive weakening but some distinctive sharpening has occurred for the amorphous band at 1271 cm^{-1}. Both results likely suggest that the amorphous chains take on the conformation similar to that of the crystalline chains; i.e., the two bands are possibly characteristic of the specific conformation adopted in the δ-form.

Previously, the in-situ IR results on the crystallization of the γ-rich phase at 65 °C have been discussed.[11a] In this research, a more detailed analysis on the IR absorption is carried out for the γ-form in comparison with the δ-form. In Figure 8a are shown the FTIR spectra of the γ-rich PHP registered at 70 °C in situ during the isothermal crystallization of PHP18K quenched from 130 °C. Similarly, from the time-resolved spectra and the second derivatives of the spectra registered at initial (0 min) and after the crystallization of 800 min shown in Figure 8b,

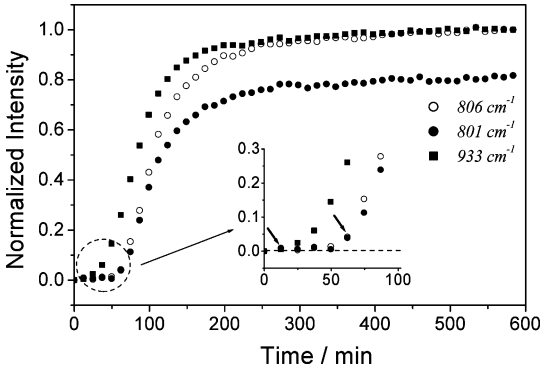

Figure 9. Normalized intensities of the splitting pairs at 806 and 801 cm^{-1} and that at 933 cm^{-1} as a function of crystallization time for PHP18K isothermally crystallizing at 70 °C after being quenched from 117 °C.

the bands can be divided into the amorphous and the crystalline bands on the origin. Unfortunately, at 70 °C, the amorphous PHP18K quenched from 130 °C shows the same IR absorption as the one quenched from 110 °C. That is, no IR evidence can be found to indicate the difference in the thermal history between them, possibly because the difference is too small to be detected by IR. The bands at 1434, 1427, 1391, 1371, 1357, 1213, 1201, 1076, 1017, 1006, 960, 806, and 801 cm^{-1}, which are absent in the spectra of the amorphous PHP, are reasonably attributed to the vibration modes of the crystalline PHP chains. The assignments are further confirmed by the difference spectra shown in Figure 8c, except for the assignment for the 1076 cm^{-1} band. As noted, the 1076 cm^{-1} band is indeed weakened rather than enhanced during crystallization, although the extent of change is not significant. With carefully inspecting the second derivative of the amorphous spectra, it is found that the line shape of the 1071 cm^{-1} band is not symmetric; i.e., a shoulder at about 1076 cm^{-1} seems to exist on its high-frequency side. On the other hand, it is also noted that the 1076 cm^{-1} band it is greatly sharpened during the crystallization. Combined all the facts, it is suggested that there are some conformational similarities between the PHP chains at amorphous state and those in the γ-form, as further confirmed by the enhancement of the two amorphous bands at 1474 and 1464 cm^{-1} during the crystallization.

In general, no common point can be found between the IR spectra of the δ- and the γ-form, suggesting the δ-form differentiates from the γ-form in the chain conformation, as will be discussed later.

As indicated by the X-ray and the POM results, when PHP18K crystallizes at 70 °C after melted at 117 °C, the growth of the γ-rich phase will suffer the competition from the δ-form crystal. Then, an in-situ IR observation was carried out here to further clarify their competitive growth. The 933 cm^{-1} band of the δ-form and the 806 and 801 cm^{-1} bands of the γ-form[11a] were monitored through the crystallization. For clarity, normalized intensity, H_s, is defined as $(H_t - H_0)/(H_\infty^s - H_0^s)$, where H_0 and H_t represent respectively the peak height of the specific band at the beginning of crystallization and that after crystallization for a time "t", and H_0^s and H_∞^s represent respectively the peak height of the standard band (the 933 cm^{-1} band for itself or the 806 cm^{-1} band for both itself and the 801 cm^{-1} band) at the beginning of crystallization and that after completion of crystallization. In Figure 9 are shown the plots of the normalized intensities for three bands as a function of the crystallization time. Obviously, the growth of the δ-form is initiated much earlier than that of the γ-rich phase, which reflects

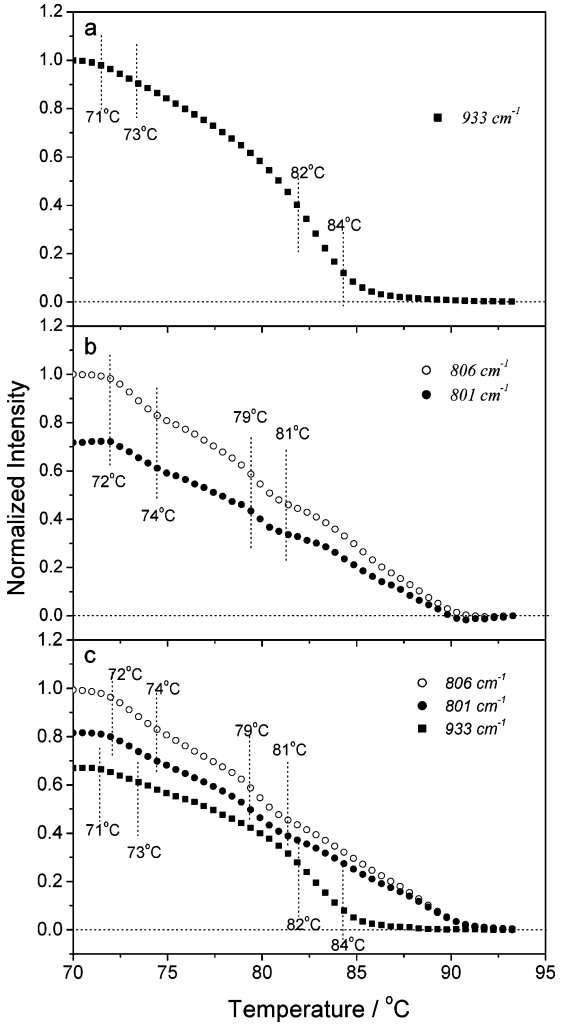

Figure 10. (a) Normalized intensities of crystalline bands at 933 cm^{-1} and/or the splitting pair at 806 and 801 cm^{-1} as a function of temperature registered during heating the PHP18K isothermally crystallized at 70 °C after being quenched from (a) 110, (b) 130, and (c) 117 °C.

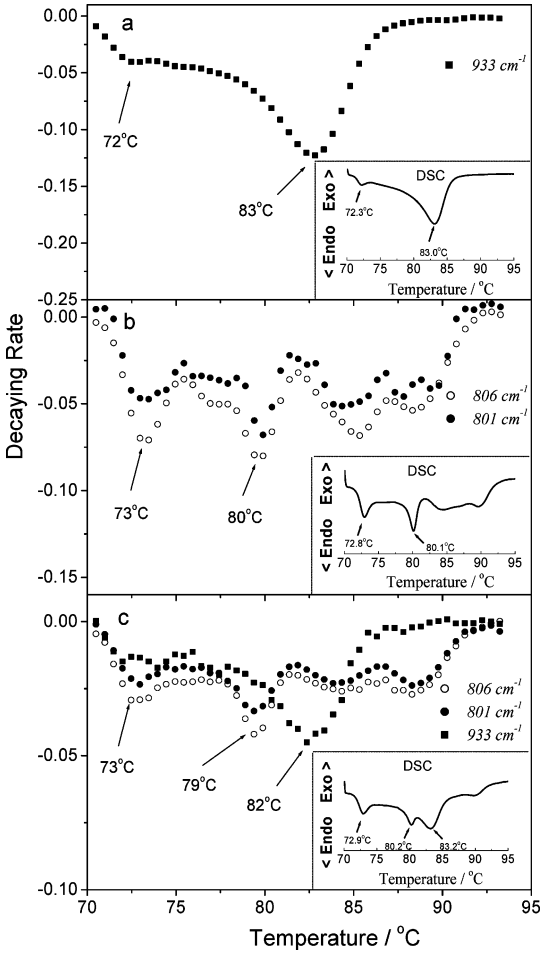

Figure 11. Decaying rates of crystalline bands at 933 cm^{-1} and/or the splitting pair at 806 and 801 cm^{-1} as a function of temperature during heating the PHP18K isothermally crystallized at 70 °C after being quenched from (a) 110, (b) 130, and (c) 117 °C. Corresponding DSC heating thermograms are inserted for comparison.

their difference in the nucleation, and is in good accord with the POM results.

Melting of δ- and γ-Form. The melting behavior of the γ-rich phase and the δ-form crystal was also monitored by tracing respectively the change of the 933 cm^{-1} band and those of the 806 and 801 cm^{-1} bands. In Figure 10 are shown the plots of the normalized intensity of the 933 cm^{-1} band and/or those of the 806 and 801 cm^{-1} pair as a function of temperature, which are registered during the heating scans of the δ-form (crystallized at 70 °C after melted at 110 °C), the γ-rich phase (crystallized at 70 °C after melted at 130 °C), and the mixed phase (crystallized at 70 °C after melted at 117 °C). It is found that the intensity of the 933 cm^{-1} band decreases quickly in the 71−73 and 82−84 °C region, where the δ-form is melted. In contrast, the paired bands of the γ-rich phase decay rapidly in the 72−74 and 79−81 °C region, where the γ-form is melted.

Similar to our previous work,[11a] a definition of the decaying rate for IR band is introduced here to describe the melting behavior more clearly. The decaying rate is defined as dH_s/dT_e, where dH_s and dT_e are respectively the small changes of the normalized intensity and the temperature with heating. Normally, the change of intensity of the crystalline band describes that of crystallinity. Therefore, the plot of the decaying rate of the crystalline band is comparable to the DSC heating thermogram. In Figure 11a−c are shown the plots of the decaying rate for the δ-form, the γ-form, and the mixed phase, which are calculated from Figure 10a−c, respectively. In addition, the corresponding DSC scans is included in each part of Figure 11 for comparison. Obviously, the plot of the decaying rate keeps accordance with the DSC heating thermogram.

As shown in Figure 11a, the heating of the δ-form displays two melting peaks at about 72 and 83 °C. It is found that the intensities and positions of the two melting peaks are both T_c- and time-dependent (not shown), and no phase transition can be detected by FTIR during the melting, possibly suggesting both are morphology-related. As for the melting of the γ-rich phase shown in Figure 11a, it display three melting peaks, i.e., two sharp ones at 73 and 80 °C and a wide one in the 84−90 °C region, which, in our previous work,[11a] are attributed to the meltings of the thin (or imperfect) phase, the major one, and the melt-recrystallized γ-form, respectively.

As shown in the DSC heating thermogram inserted in Figure 11c, the melting of the mixed phase is very complex, which shows four melting peaks at 73, 80, 83, and 90 °C. Fortunately, as shown in Figure 11c, the melting of the mixed phase can be simply resolved into those of the δ- and γ-form via monitoring the decaying rate of the 933 cm^{-1} band and those of the 806 and 801 cm^{-1} pair. Then, the multimelting behavior of the mixed phase can be explained reasonably. In addition, we compare the melting behavior of the δ-form and the γ-rich phase in the mixed phase with that of the pure phase and find no difference.

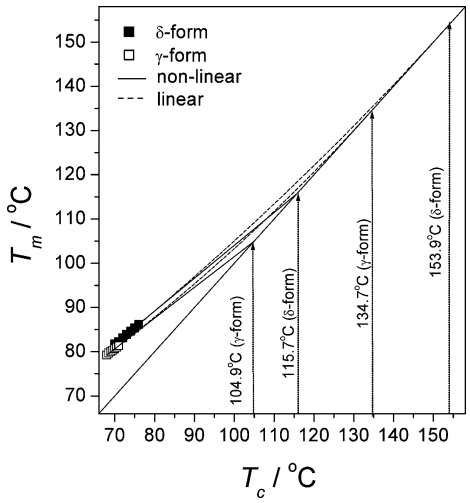

Figure 12. Extrapolation of melting temperatures with crystallization temperatures, analyzed with the linear and nonlinear approaches for the initial lamellae of the δ- and γ-form.

It seems that the δ-form and the γ-rich phase in the mixed phase are melted isolatedly; i.e., no phase transition occurs between them during heating.

Thermal Stability of Two Crystals. It would be helpful for us to understand the polymorphism of PHP if the equilibrium melting temperature (T_m^0) of the two phases can be compared. Recently, the validity of the linear Hoffman−Weeks extrapolation to determine T_m^0 has been critically reviewed by Marand et al.[12] Their results indicated that, first, the linear extrapolation is not justified on the theoretical grounds, as it holds only at extremely low supercoolings, which are not experimentally accessible; second, the linear extrapolation leads to underestimation of T_m^0 and overestimation of the thickening coefficient. Thus, the nonlinear extrapolation developed by Marand et al.[12] is applied here. In this experiment, the δ- and γ-phase are isothermally formed respectively at 70−74 °C after melting at 110 °C and at 68−72 °C after melting at 130 °C. The f2 fraction of PHP70K is used to prepare the γ-form instead of the PHP18K, as the higher MW favors the growth of the γ-form crystal.[11a]

The details about the nonlinear approach will not be involved here, as it has been well addressed in many works.[12] To avoid complications in the analysis caused by thickening, we used the melting temperature of initial (nonthickened) lamellae, which is obtained by extrapolating the measured peak melting temperatures to zero crystallinity. The extrapolated melting points of the δ- and γ-form are plotted as a function of the T_c value in Figure 12. For comparison, the linear Hoffman−Weeks plots are included. The T_m^0 values determined by the linear and nonlinear Hoffman−Weeks plots are respectively 104.9 and 134.7 °C for the γ-form, and 115.7 and 153.9 °C for the δ-form. It is quite clear that the linear and nonlinear extrapolations lead to significantly different estimates on T_m^0, the latter being about 30 °C higher.

However, the T_m^0 of the δ-form is always higher than that of the γ-form, whether the linear or nonlinear extrapolation is employed. On the basis of the thermodynamic equilibrium, the chemical potentials of polymer repeating unit in the crystal and in the melt must be equal at equilibrium. The melting temperature is defined as the ratio of the heat of fusion, ΔH_m, to the entropy of fusion, ΔS_m (i.e., $T_m^0 = \Delta H_m/\Delta S_m$). As a matter of fact, the higher value of T_m^0 in the δ-form may be attributed to the lower value of ΔS_m and/or the higher value of ΔH_m. In other words, the Gibbs free energy, $G_c = H_c - TS_c$, of the δ-form is lower than the γ-form, indicating the higher thermal stability of the δ-form than the γ-form.

Discussion

2_1 Helix Conformation in δ-Form. In our previous work,[11a] a tentative assignment has been made to clarify the IR spectra of the γ-form PHP, which is based on the reports on PHP[8a] and with referring to those on polyethylene (PE),[13] poly(ethylene glycol) (PEG),[14] the related polyesters with the ethylene glycol unit,[15] poly(ϵ-caprolactone),[16] etc. A similar assignment is also carried out here for the IR absorption of the δ-form as following: the crystalline bands at 1458, 1409, and 1400 cm^{-1}, those at 1389 and 1375 cm^{-1}, those at 1271, 1222, and 1208 cm^{-1}, those at 1022, 1010, and 999 cm^{-1}, and that at 933 cm^{-1} are attributed to the CH_2 bending, the CH_2 wagging, the C−O−C stretching, the C−C stretching, and the CH_2 rocking, respectively. These vibration modes are known to be very sensitive to the conformation adopted by polymer chains.[13−16] Therefore, the fact that the IR spectrum of the δ-form is not the same as that of the γ-form at all unambiguously indicates that the δ-form PHP does not take on the same trans conformation as the γ-form one. The previous conformational analysis[9] predicted that PHP and the α- or β-substituted PHPs would crystallize in either the 2_1 helix or the trans conformation alternatively. Up to date, this prediction has been well validated without exception by all the research on PHP,[8] PHB,[6] polypivalolactone,[10a−c] poly(α-methyl-α-*n*-propyl-β-propiolactone),[10d,e] and poly(α-methyl-α-ethyl-β-propiolactone).[10e−g] As a result, it is reasonable that the PHP chains in the δ-form are 2_1 helix conformed; i.e., C(═O)−CH_2−CH_2−O−C(═O) segments adopt the GGTT conformation.

A detailed IR analysis would shed more light on the conformation of the δ-form PHP. First, let us focus on the CH_2 bending vibration, which is sensitive to the conformation of ethylene group. For PE,[13] PEG,[14a] poly(ethylene 2,6-naphthalate) (PEN),[15a−c] and poly(ethylene terephthalate) (PET),[15a] the CH_2 bending of the trans ethylene group and that of the gauche one are calculated and/or observed to show IR absorption in the 1485−1470 and 1465−1455 cm^{-1} regions, respectively. It is then reasonable to attribute the 1474 and/or 1464 cm^{-1} band of the γ-form to the trans-conformed ethylene group. In contrast, the appearance of a CH_2 vibration band at 1458 cm^{-1} in the spectra of the δ-form likely indicates that the ethylene group is gauche-conformed in the δ-form.

Normally, the CH_2 wagging modes of the gauche and the trans-conformed ethylene group of PEG induce respectively two IR absorption at about 1360 and 1340 cm^{-1}.[14a] In addition, the corresponding gauche and the trans bands are at 1370 and 1337 cm^{-1} for PEN[15a−c] and 1365 and 1337 cm^{-1} for PET.[15a] Thus, the 1375 cm^{-1} band of the δ-form and the 1343 cm^{-1} band of the γ-form possibly reflect respectively the gauche ethylene in the δ-form and the trans one in the γ-form.

Furthermore, the CH_2 rocking is also quite dependent on the backbone conformation. The GGT-conformed ethylene glycol of PEG is computed and observed to show a CH_2 rocking band at around 920 cm^{-1}. The corresponding gauche rocking bands for PEN[15a−c] and PET[15a,f] are found to be around 930 cm^{-1}. Namely, the presence of the 933 cm^{-1} band possibly implies the gauche conformation of the ethylene group in the δ-form. On the other hand, the trans-conformed ethylene glycol gives birth to the 848 cm^{-1} band for PET[15a] and the 813 cm^{-1} band for the α-form (all-trans) PEN.[15a,c] Thus, the absorption around

804 cm^{-1} of the γ-form possibly arises from the trans-conformed PHP chains. Actually, the CH_2 rocking absorptions of the γ-form around 804 cm^{-1} split into two bands at 806 and 801 cm^{-1} due to the strong intermolecular interaction in the γ-form.[11a] The crystal-field splitting possibly produces another pair of bands at 1434 and 1427 cm^{-1} for the γ-form.[11a]

As previously indicated, the C−O stretching band at 1271 cm^{-1} arises from the amorphous PHP. It is not strange at all to note its absence in the IR spectra of the γ-form. However, it is really notable that the 1271 cm^{-1} band is still present in the IR spectra of the δ-form, which, as shown in Figure 7, is almost not weakened but greatly sharpened with crystallization. In other words, the 1271 cm^{-1} band reflects the conformation adopted in the δ-form. As the isotactic PHB shares the same backbone with PHP, the backbone vibration of PHB and PHP should show similar IR absorption when they conformed similarly. It is reported that the C−O stretching bands at 1279 and 1228 cm^{-1} are characteristic of the 2_1 helix conformation for PHB.[17] In this way, the presence of the two C−O stretching bands at 1271 and 1222 cm^{-1} in the IR spectra tends to indicate that the PHP chains adopt the 2_1 helix in the δ-form.

Actually, the difference of the conformation explains only partially the spectral difference between the two crystal forms. The packing way in the crystal also affect the IR absorption and is possibly responsible for the appearance of new bands in the most of cases. In our previous work,[11a] the split absorptions around 1430 and 804 cm^{-1} are attributed to the tight packing of PHP chains in the γ-form. In this research, with the aid of the difference spectra and the subtraction spectra, the crystal-field splitting is also clearly observed for the CH_2 wagging mode at 1365 cm^{-1}, which splits into 1371 and 1356 cm^{-1} bands, and the C−C stretching band at 1008 cm^{-1}, which splits into 1017 and 1006 cm^{-1} bands. For the δ-form, no new bands and thus no IR splitting have been observed in the same vibration region, possibly indicating that the δ-form is not packed so tightly. However, the two C−C stretching bands at 1010 and 1022 cm^{-1} and the two CH_2 wagging bands at 1409 and 1400 cm^{-1} are really look like pairs of bands corresponding to one single amorphous band. As the PHP chains adopt the 2_1 helix conformation in the δ-form, the band pairs possibly arise from the intramolecular helical splitting.[18]

Several amorphous bands are found to be characteristic of the crystalline structure, which possibly indicates the corresponding group in the amorphous phase adopting the same conformation as that in the crystalline phase. That is, the amorphous CH_2 vibration band at 1458 cm^{-1} and those at 1474, 1464, and 1343 cm^{-1} possibly arisen from the gauche- and the trans-conformed ethylene group in the amorphous phase, respectively. In addition, the amorphous C−O stretching band at 1271 cm^{-1} possibly corresponds to the TT-conformed $-CH_2-O-C(=O)-$ in the amorphous phase.

Driving Force To Form δ-Form. i. Cast PHP. It is known that with decreasing the MW value the crystalline structure of the cast PHP changes in the order of γ-form, β-form, and δ-form. However, the fundamental issue of the driving force leading to the MW-dependent polymorphism, and especially the formation of the δ-form, still remains open.

During the past several years, the influence of MW on the crystallization of polymers is intensely concerned.[19] As usual, the MW-dependent polymorphism arises from either the kinetic reason or the thermodynamic one. From a view of kinetic, a decrease of MW, resulting in the increased chain mobility and the depressed T_m^0, possibly increases or decreases the crystallization rates of the various crystal forms. But, since the extent of this change may be different, it may destabilize some chain conformation or some kinds of packing compared to the other ones. Possibly, the competition between the growths of polymorphic crystals depends more on the change of the T_m^0 than that of the mobility, as the contribution from the change of the mobility to the growth of each crystal is normally similar. In this way, the less thermodynamically accessible but kinetically more stable form possibly crystallizes faster in the polymer with lower MW, making its amount preponderant over the more thermodynamically accessible one, which seemingly happens in poly(decamethylene oxide)[19c] and poly(pentene-1).[19g] On the other hand, from a thermodynamic viewpoint, as the chain ends will hardly enter into the crystal, the chain ends, with decreasing MW (increasing relative amount of chain ends), will tend to accumulate preferentially at the crystalline−amorphous interface and will perturb the crystalline morphology much less in a situation with the large crystal surface per chain.[19b] Namely, the chain ends are viewed as the defects similar to the comonomeric units and the stereoirregular segments in polymers.

As revealed by us, the β-form crystal, as a kinetically stable phase,[11a] is favored in both the melt-crystallized[11a] and the cast PHPs with lower MW. In addition, the lamellar thickness of the melt-crystallized β-form PHP is similar to that of the melt-crystallized γ-form PHP, as indicated by the small-angle X-ray scattering results (not shown here). Thus, it seems reasonable that the growth of the β-form crystal in PHPs with low MW is due to the kinetic force rather than the thermodynamic one.

As to the δ-form crystal, it is also of interest that it only grows in the PHP with MW below 5.6×10^4. Unfortunately, at any T_c, we cannot detect any evidence showing the presence of the δ-form crystal in the melt-crystallized PHP with low MW after melted at above 130 °C, suggesting that the kinetic force is not or only partially responsible for the formation of the δ-form. The cast δ-form holds a similar lamellar thickness to the cast γ-form (not shown here), which also likely excludes the possibility that the formation of the δ-form is due to the large crystal surface per chain of the δ-form. In fact, the absence of the δ-form in the random poly(3-hydroxybutyrate-*co*-3-hydroxypropionate) with very low content of 3-hydroxybutyrate units[20] again excludes the defect effect of the end group as a possible reason.

However, we still speculate that the formation of the δ-form crystal is related to the terminal groups of PHP. As revealed by NMR (not shown here), our PHP samples hold two kinds of terminal groups, i.e., the carboxylic acid and the hydroxyl groups. Similar to the hydroxyl groups of poly(ethylene oxide),[21] those terminal groups of PHP likely interact with each other via the hydrogen bond, especially in the low-molecular-weight PHP. It is expected that the intramolecular association is more favorable than the intermolecular association because of the low concentration range in this research and the use of the chloroform (good solvent for PHP). In fact, the solvent is very important for the formation of the δ-form. Our most recent result indicates that the good solvent benefits the formation of the δ-form (not shown). The intramolecular association may prevent the chains from adopting some conformation or trap the chains into some specific conformations during the crystallization. The restrictive effect of the hydrogen bonds on the crystallization during the precipitation from the concentrated solution renders it of interest to clarify the effect of the hydrogen bonds on the polymorphism.

ii. Melt-Crystallized PHP. In Figure 13 are shown the DSC cooling scans at 10 °C/min for PHP18Ks melted at various temperatures. It is obvious that the lower T_f upshifts the

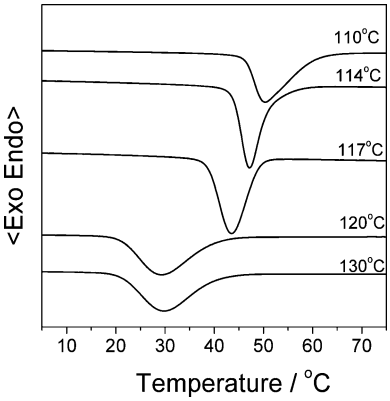

Figure 13. DSC cooling scans for PHP18Ks melted at 110, 114, 117, 120, and 130 °C.

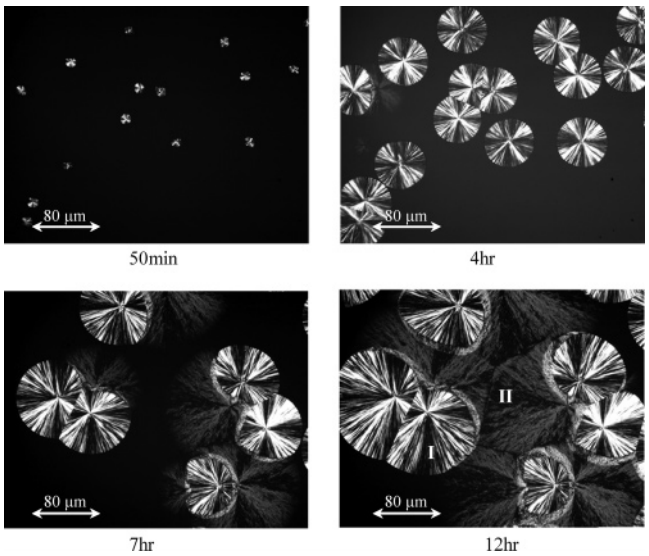

Figure 14. Optical microphotographs of spherulites growing in PHP18Ks at 70 °C after being quenched from 117 °C. Type I and II spherulites correspond to the δ-form and the γ-rich phases, respectively.

crystallization temperature, indicating the density of the heat-sensitive nuclei increases with decreasing T_f, which is well accordant with the POM results. However, such heat-sensitive nuclei cannot survive at the temperature as high as 120 °C, as the PHP18K hold the same crystallization kinetics after melted at any T_f above 120 °C.

As shown in Figure 6, the δ-form grows much slower than the γ-rich crystal at 70 °C. Thus, the overwhelming preponderant growth of the δ-form after melting at 110 °C implies the heat-sensitive nuclei would intend to nucleate the δ-form rather than the γ- and β-form. In addition, it is noted that once the PHP18K is melted at 130 °C, no δ-form is formed during the melt-crystallization,[11a] suggesting that the δ-form is only nucleated by the heat-sensitive nuclei. On the contrary, the nucleation of the γ-rich crystal shows an inverse dependence on the T_f, suggesting that the γ- and β-form cannot be nucleated by the heat-sensitive nuclei at all.

In fact, the different nucleation mechanisms of crystals are also reflected by the competitive growth of two crystal forms. In Figure 14 are shown the POM photographs of the PHP18K quenched to 70 °C after melted at 117 °C, which are arranged in the crystallization time. The latter two photographs were taken from a different place in the same sample. As shown in the first two photographs, the δ-form nucleates much earlier than the γ-rich (about 50 min earlier), as is also evidenced by the corresponding in-situ IR (Figure 9) and the DSC cooling scan at 1 °C/min after melting at 117 °C (not shown). It obviously indicates that the residual heat-sensitive nuclei can nucleate the δ-form very effectively. In addition, all the δ-form spherulites are found to nucleate almost simultaneously, and no additional nucleation occurs for the δ-form during the subsequent process, suggesting that the nucleation of the δ-form is not time-dependent and hence heterogeneous. Thus, it is not strange to note that all the δ-form spherulites have almost the same size before impingements. In contrast, the nucleation of the γ-rich is continuous and time-dependent. In addition, as revealed by the in-situ FTIR (not shown), the induction time for the crystallization of the γ-form after melting at 117 °C is comparable to that after melting at 130 °C, indicating that the nucleation of the γ-rich is insensitive to the residual heat-sensitive nuclei (denoted as the δ-nuclei from now on).

It is reasonable that the residual heat-sensitive nuclei make a difference between the nucleations of the two kinds of crystals, as the heat-sensitive nuclei are quite possibly some residual chain orders of the δ-form. However, it is still amazing to note that the heat-sensitive nuclei can withstand such a high temperature (117 °C), which is about 34 °C higher than the melting temperature of the δ-form (83 °C). The residual chain orders should not be partially melted lamella but at most some small crystal fragments. In fact, the residual chain orders should be very short, as it cannot be detected by FTIR (Figures 7 and 8) at all. Moreover, it is noted that the self-nucleation domain of the cast PHP18K (not shown), where no partially melted lamella exists, almost locates in the same T_f range as that where a strong T_f-dependent polymorphism is found.

The density of such δ-nuclei is dependent only on the T_f value and the annealing time. In other words, the density of the δ-nuclei should be similar after melting at the same T_f for the same time and lead to the fixed nucleation of the δ-form independent of the T_c value. On the other hand, the nucleations of the γ- and/or β-form would increase with decreasing T_c from 70 °C.[11a] Thus, the competition between the nucleations of various crystals does play an important role in the T_c-dependent polymorphism of PHP.

Kinetically Favored But Thermally More Stable. Normally, the less thermally stable phase, with the introduction of its specific nuclei, can preponderate over the thermally stable one even at a very high temperature.[22] Thus, it is not strange at all to find that the δ-form, the thermally more stable phase, becomes the major phase via heterogeneously nucleating on the residual heat-sensitive δ-nuclei. However, it is really remarkable that no evidence could be available to indicate the spontaneous melt-crystallization of the δ-form without the δ-nuclei. That is, once the δ-phase is melted at or above 120 °C, no δ-form but the γ- or β-form can be formed.[11a] Until now, no reasonable explanation can be available to be responsible for the absence of the spontaneous nucleation of the thermally most stable phase, i.e., the δ-form, during the melt-crystallization.

Conclusion

A new crystal form, i.e., the δ-form, has been prepared in the cast and the melt-crystallized low-MW PHP by optimizing the crystallization conditions. It has been found that the crystalline structure of cast PHPs quite depends on the MW. With decreasing the MW, the crystalline structure of cast PHPs changes on the order of γ-, β-, and δ-form. The kinetic force and the restrained conformation by the intramolecular interaction are proposed to give birth to respectively the β- and δ-form in the low-MW PHP. For melt-crystallized low-MW PHPs, both T_f and T_c are found to be quite effective factors to control their

crystalline structures. A low T_f and a high T_c favor the formation of the δ-form, a high T_f and a high T_c favor the formation of the γ-form, and a low T_c favors that of the β-form. The complex T_f- and T_c-dependent polymorphism of low-MW PHP is suggested to be related to the different nucleation mechanisms of the β-, γ-, and δ-form. The δ-form only heterogeneously nucleates on the heat-sensitive δ-nuclei, whose density only relies on the T_f under a fixed annealing time. In contrast, the nucleation of the mixed phase of the γ- and β-form is T_c-dependent and not sensitive to the δ-nuclei. The T_f-dependent nucleation of the δ-form competes with the T_c-dependent one of the other polymorphic crystals and plays a very important part in the T_f- and T_c-dependent polymorphism of low-MW PHP.

Being different from the trans-conformed PHP chains in the γ- and β-form, the PHP chains in the δ-form have been suggested to take on the 2_1 helix conformation, i.e., the most usual one for the crystalline P3HAs, by the FTIR analysis and the conformation prediction. With in-situ tracing the conformational bands, the multiple-melting behavior of the δ-form and the other polymorphic crystals have been clarified. It is found that the δ-form and the γ-rich phase, which coexist in one sample, are melted without affecting the structure evolution each other, although the δ-form is found to be thermally more stable and have a higher melting temperature than the γ-form.

References and Notes

(1) (a) Doi, Y. In *Microbial Polyesters*; VCH Publishers: New York, 1990. (b) Inoue, Y.; Yoshie, N. *Prog. Polym. Sci.* **1992**, *17*, 571. (c) Yoshie, N.; Inoue, Y. In *Biopolymers*; Steinbüchel, A., Ed.; Wiley-VCH: Weinheim, 2001; Vol. 3, Chapter 6. (d) Feng, L.; Yoshie, N.; Asakawa, N.; Inoue, Y. *Macromol. Biosci.* **2004**, *4*, 186.

(2) (a) Baba, H.; Tanahashi, N.; Kumagai, Y.; Doi, Y. *J. Chem. Soc. Jpn.* **1992**, *5*, 527. (b) Spyros, A.; Kimmich, R.; Briese, B. H.; Jendrossek, D. *Macromolecules* **1997**, *30*, 8218. (c) Scandola, M.; Focarete, M. L.; Gazzano, M.; Matuszowicz, A.; Sikorska, W.; Adamus, G.; Kurcok, P.; Kowalczuk, M.; Jedlinski, Z. *Macromolecules* **1997**, *30*, 7743. (d) He, Y.; Shuai, X.; Kasuya, K.; Doi, Y.; Inoue, Y. *Biomacromolecules* **2001**, *2*, 1045. (e) Koyama, N.; Doi, Y. *Macromolecules* **1997**, *30*, 826. (f) Cao, A.; Arai, Y.; Yoshie, N.; Kasuya, K.; Doi, Y.; Inoue, Y. *Polymer* **1999**, *40*, 6821.

(3) Abe, H.; Doi, Y.; Aoki, H.; Akehata, T. *Macromolecules* **1998**, *31*, 1791.

(4) (a) Wunderlich, B.; Grebowicz, J. *Adv. Polym. Sci.* **1984**, *60/61*, 1. (b) Tonelli, A. E.; Gomez, M. A.; Tanaka, H.; Schilling, F. C.; Cozine, M. H.; Lovinger, A. J.; Bovey, F. A. *Adv. Chem. Ser.* **1990**, *227*, 409. (c) Corradini, P.; Guerra, G. *Adv. Polym. Sci.* **1992**, *100*, 183. (d) Woo, E. M.; Sun, Y. S.; Yang, C.-P. *Prog. Polym. Sci.* **2001**, *26*, 945. (e) Gorrasi, G.; Guadagno, L.; D'Aniello, C.; Naddeo, C.; Romano, G.; Vittoria, V. *Macromol. Symp.* **2003**, *203*, 285.

(5) (a) Lovinger, A. J.; Schilling, F. C.; Bovey, F. A.; Zeigler, J. M. *Macromolecules* **1986**, *19*, 2657. (b) Meille, S. V.; Ferro, D. R.; Bruckner, S.; Lovinger, A. J.; Padden, F. J. *Macromolecules* **1994**, *27*, 2615. (c) Ho, R.-M.; Cheng, S. Z. D.; Hsiao, B. S.; Gardner, K. H. *Macromolecules* **1995**, *28*, 8855. (d) Lotz, B.; Wittmann, J. C.; Lovinger, A. J. *Polymer* **1996**, *37*, 4979. (e) Hsiao, B. S.; Kreuz, J. A.; Cheng, S. Z. D. *Macromolecules* **1996**, *29*, 135. (f) Varga, J.; Ehrenstein, G. W. *Colloid Polym. Sci.* **1997**, *275*, 511. (g) Kellera, A.; Cheng, Stephen, Z. D. *Polymer* **1998**, *39*, 4461. (h) Vittoria, V.; Guadagno, L.; Comotti, A.; Simonutti, R.; Auriemma, F.; De Rosa, C. *Macromolecules* **2000**, *33*, 6200. (i) Andruzzi, L.; D'Apollo, F.; Galli, G.; Gallot, B. *Macromolecules* **2001**, *34*, 7707. (j) De Rosa, C.; Auriemma, F.; Ruiz de Ballesteros, O. *Macromolecules* **2004**, *37*, 1422.

(6) (a) Yokouchi, M.; Chatani, Y.; Tadokoro, H.; Teranishi, K.; Tani, H. *Polymer* **1973**, *14*, 267. (b) Orts, W. J.; Marchessault, R. H.; Bluhm, T. L.; Hamer, G. K. *Macromolecules* **1990**, *23*, 5368. (c) Iwata, T.; Aoyagi, Y.; Fujita, M.; Yamane, H.; Doi, Y.; Suzuki, Y.; Takeuchi, A.; Uesugi, K. *Macromol. Rapid Commun.* **2004**, *25*, 1100.

(7) (a) Eling, W. B.; Gogolewski, S.; Pennings, A. J. *Polymer* **1982**, *23*, 1587. (b) Hoogsteen, W.; Postema, A. R.; Pennings, A. J.; Ten Brinke, G.; Zugenmaier, P. *Macromolecules* **1990**, *23*, 634.

(8) (a) Wasai, T.; Saegusa, T.; Furukawa, J. *Kogyo Kagaku Zasshi* (*J. Chem. Soc. Jpn., Ind. Chem. Sect.*) **1964**, *67*, 601. (b) Suehiro, K.; Chatani, Y.; Tadokoro, H. *Polym. J.* **1975**, *7*, 352. (c) Furuhashi, Y.; Iwata, T.; Sikorski, P.; Atkins, E.; Doi, Y. *Macromolecules* **2000**, *33*, 9423. (d) Furuhashi, Y.; Iwata, T.; Kimura, Y.; Doi, Y. *Macromol. Biosci.* **2003**, *3*, 462.

(9) (a) Cornibert, J.; Marchessault, R. H. *Macromolecules* **1975**, *8*, 296. (b) Cornibert, J. Ph.D. Thesis, Université de Montréal, 1972.

(10) (a) Perego, G.; Melis, A.; Cesari, M. *Makromol. Chem.* **1972**, *157*, 269. (b) Prud'homme, R. E.; Marchessault, R. H. *Macromolecules* **1974**, *7*, 541. (c) Meille, S. V.; Konishi, T.; Geil, P. H. *Polymer* **1984**, *25*, 773. (d) Cornibert, J.; Marchessault, R. H.; Allegrezza Jr., E. A.; Lenz, R. W. *Macromolecules* **1973**, *6*, 676. (e) He, Z.; Prud'homme, R. E. *Macromolecules* **1999**, *32*, 7655. (f) Grenier, D.; Prud'homme, R. E. *Macromolecules* **1983**, *16*, 302. (g) Duchesne, D.; Prud'homme, R. E. *Polymer* **1979**, *20*, 1199.

(11) (a) Zhu, B.; He, Y.; Asakawa, N.; Yoshie, N.; Nishida, H.; Inoue, Y. *Macromolecules* **2005**, *38*, 6455. (b) Zhu, B.; He, Y.; Asakawa, N.; Yoshie, N.; Nishida, H.; Inoue, Y. *Macromol. Rapid Commun.* **2005**, *26*, 581.

(12) (a) Marand, H.; Xu, J.; Srinivas, S. *Macromolecules* **1998**, *31*, 8219. (b) Xu, J.; Srinivas, S.; Marand, H. *Macromolecules* **1998**, *31*, 8230.

(13) Krimm, S.; Liang, C. Y.; Sutherland, G. B. B. M. *J. Chem. Phys.* **1956**, *25*, 549.

(14) (a) Matsuura, H.; Miyazawa, T. *J. Polym. Sci.* **1969**, *7*, 1735. (b) Li, X.; Hsu, S. L. *J. Polym. Sci., Part B* **1984**, *22*, 1331.

(15) (a) Quchi, I.; Hosoi, M.; Shimotsuma, S. *J. Appl. Polym. Sci.* **1977**, *21*, 3445. (b) Kimura, F.; Kimura, T.; Sugisaki, A.; Komatsu, M.; Sata, H.; Ito, E. *J. Polym. Sci., Polym. Phys. Ed.* **1997**, *35*, 2741. (c) Vasanthan, N.; Salem, D. R. *Macromolecules* **1999**, *32*, 6319. (d) Ward, I. M. *Chem. Ind. London* **1956**, 905. (h) Ward, I. M. *Chem. Ind. London* **1957**, 1102. (e) Miyake, A. *J. Polym. Sci.* **1959**, *38*, 479. (f) D'Espositio, L.; Koenig, J. L. *J. Polym. Sci., Polym. Phys. Ed.* **1976**, *14*, 1731. (g) Lin, S.-B.; Koenig, J. L. *J. Polym. Sci., Polym. Phys. Ed.* **1982**, *20*, 2277.

(16) (a) Holland-Moritz, K.; Hummel, D.-O. *J. Mol. Struct.* **1973**, *19*, 289. (b) Holland-Moritz, K.; Siesler, H.-W. *Appl. Spectrosc. Rev.* **1976**, *11*, 1.

(17) (a) Sato, H.; Murakami, R.; Padermshoke, A.; Hirose, F.; Senda, K.; Noda, I.; Ozaki, Y. *Macromolecules* **2004**, *37*, 7203. (b) Xu, J.; Guo, B.-H.; Yang, R.; Qiong, W.; Chen, G.-Q.; Zhang, Z.-M. *Polymer* **2002**, *43*, 6893.

(18) Koenig, J. L. In *Spectroscopy of Polymer*; American Chemical Society: Washington, DC, 1992.

(19) (a) Alamo, R. G.; Kim, M.-H.; Galance, M. J.; Isasi, J. R.; Mandelkern, L. *Macromolecules* **1999**, *32*, 4050. (b) Brückner, S. *Macromol. Rapid Commun.* **1997**, *18*, 1. (c) Baltá Calleja, F. J.; Bermudez, S. F. *J. Appl. Crystallogr.* **1974**, *7*, 506. (d) Morrow, D. R.; Newman, B. A. *J. Appl. Crystallogr.* **1968**, *39*, 4944. (e) Meille, S. V.; Romita, V.; Caronna, T.; Lovinger, A. J.; Catellani, M.; Belobrzeckaja, L. *Macromolecules* **1997**, *30*, 7898. (f) Medellín-Rodríguez, F. J.; Larios-López, L.; Zapata-Espinoza, A.; Dávalos-Montoya, O.; Phillips, P. J.; Lin, J. S. *Macromolecules* **2004**, *37*, 1799. (g) Danusso, F.; Gianotti, G. *Makromol. Chem.* **1963**, *61*, 164. (h) Rodriguez-Arnold, J.; Zhang, A.; Cheng, Stephen, Z. D.; Lovinger, A. J.; Hsieh, E. T.; Chu, P.; Johnson, T. W.; Honnell, K. G.; Geerts, R. G. *Polymer* **1994**, *35*, 1884. (i) Kojima, M. *J. Polym. Sci., Part B* **1967**, *5*, 245. (j) Kojima, M. *J. Polym. Sci., Part A-2* **1968**, *6*, 1255. (k) Morrow, D. R.; Newman, B. A. *J. Appl. Phys.* **1968**, *39*, 4944. (l) Lotz, B.; Graff, S.; Wittman, J. C. *J. Polym. Sci., Polym. Phys. Ed.* **1986**, *24*, 2017.

(20) Cao, A.; Asakawa, N.; Yoshie, N.; Inoue, Y. *Polymer* **1998**, *39*, 4801.

(21) Shimada, T.; Okui, N.; Kawai, T. *Makromol. Chem.* **1980**, *181*, 2643.

(22) (a) Ho, R. M.; Lin, C. P.; Tsai, H. Y.; Woo, E. M. *Macromolecules* **2000**, *33*, 6517. (b) Sun, Y. S.; Woo, E. M. *Macromolecules* **1999**, *32*, 7836.

MA051922V